V-GRAM

Magellan Bulletin About Venus and the Radar Mapping Mission

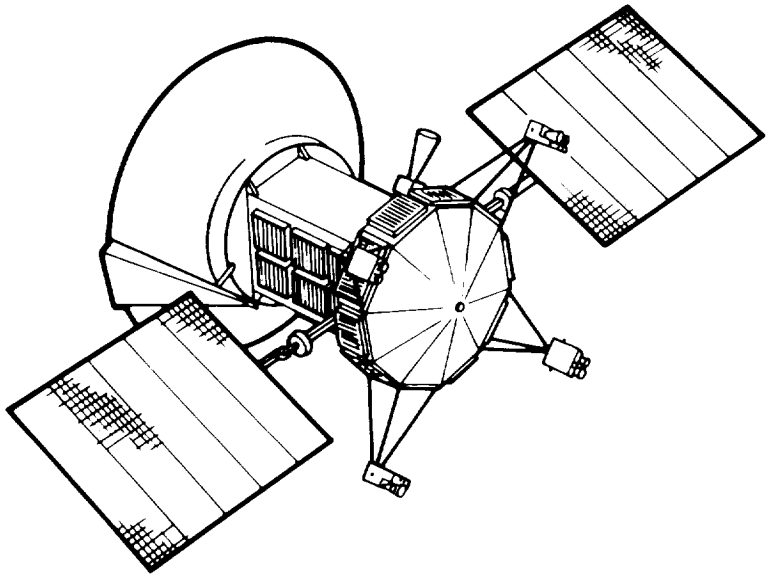

APRIL 1993

Jet Propulsion Laboratory
California Institute of Technology
Pasadena, CA

V-GRAM

Issue No. 20 April 1993

Magellan Project Manager: Douglas G. Griffith

Magellan Project Scientist: R. Stephen Saunders

V-Gram Editor: Mona Jasnow

TABLE OF CONTENTS

Published by the Magellan Project, Jet Propulsion Laboratory, California Institute of Technology. For information, contact Mona Jasnow, Jet Propulsion Laboratory, Mail Stop 230-225, 4800 Oak Grove Drive, Pasadena, CA 91109. (818) 393-1001. NASAmail: MJASNOW

MAGELLAN PROJECT UPDATE

Thomas W. Thompson
Magellan Science Manager

Much has happened since the last *V-Gram*, in July 1991. The second mission cycle, from mid-May 1991 through mid-January 1992, was successful in acquiring radar images for 54% of the planet. Cumulative planet coverage, which was 84% at the end of the first mission cycle, rose to 96% at the end of the second mission cycle and 98% at the end of the third, when imaging was stopped. The remaining tape recorder performed flawlessly. In addition, the "loss-of-signal" events were traced to a subtle bug in the flight software. That bug was fixed in early July 1991, and no more of these "loss-of-signal" events have occurred since.

Mission Cycle 2 was conducted in that portion of the Venus orbit where operations were affected by the geometry relative to the Sun. In particular, the spacecraft electronic bays were heated by solar illumination during the data playbacks, which occupy two hours of each 3.25-hour orbit. The spacecraft was cooled by pointing the large high-gain antenna toward the Sun to shade the rest of the spacecraft. Since data on the tape recorder cannot be relayed to Earth during these Sun-pointing periods, the typical mapping swath in Cycle 2 was about half that for the first mission cycle. Most of the southern half of Venus was mapped in a right-looking geometry, allowing southern areas not mapped in the first mission cycle to be seen for the first time during Cycle 2. Areas mapped in the first mission cycle were observed for a second time in a right-looking geometry that complemented the left-looking geometry of the first cycle.

A successful stereo test in mid-Cycle 2 pointed the way for Mission Cycle 3. An 8-orbit test on July 24, 1991, showed that Magellan could revisit mapped areas with a different left-looking geometry and create the equivalent of photogrammetric stereo pairs (similar to a standard Earth mapping technique that uses multiple photographs from high-flying aircraft). Thus, the objective for the third mission cycle (mid-January to mid-September 1992) was to obtain as much stereo coverage of Venus as the spacecraft and ground systems would allow. Stereo image data are discussed further in the accompanying article by Jeff Plaut, "Magellan Stereo Image Data."

The end of Mission Cycle 2 was punctuated by a failure of the downlink transponder on January 4, 1992. Transponder A failed such that the downlink X-band signal had no modulation; no high-rate radar data could be transmitted back to Earth. The radar data playback was switched to the backup Transponder B (Tx-B), which had been used until March 1991, when it had deteriorated. Radar data downlinks with Tx-B during the third mission cycle, from mid-January until mid-September 1992, had both successes and failures. In February and March, Tx-B transmitted good data at 115 kilobits/second instead of 268 kilobits/second, when the transponder was at high and constant temperatures. In April, the spacecraft passed through the shadow of Venus during the apoapsis portion of the orbit, when Magellan travels relatively slowly. The spacecraft was shaded for up to 58 minutes in each 3.25-hour orbit. Since Magellan was first heated by the Sun and then plunged into total darkness, the spacecraft temperatures could not be stabilized. The transponder performance deteriorated and data were lost until these solar occultations passed. About three weeks later, in early May, personnel at the Deep Space Network (DSN) discovered that small changes in receiver phase lock loops greatly improved our ability to capture the relatively weak signals that Magellan was broadcasting. The combination of constant temperatures and the ground phase adjustments resulted in the collection of good radar data.

Successful downlinks lasted until early June (mid-Cycle 3), when Venus entered its second superior conjunction. Venus and the Magellan spacecraft passed behind the Sun for 36 hours on June 12–14. Previous experience with our first superior conjunction in October and November 1990, however, indicated that we could not communicate reliably with the spacecraft, and radar operations were suspended for the first three weeks of June 1992. Although good downlinks were being obtained until we ceased operations for superior conjunction, the transponder mysteriously deteriorated during those three weeks when mapping was suspended. Routine radar mapping was not possible when operations were restarted in early July. Only a few passes with DSN's large-aperture 70-m antennas were obtained; an area near the Stowe crater was successfully observed. This was an area that appeared significantly different in the left-look images versus right-look ones. The Cycle 3 views matched the Cycle 1 images, confirming that the Venusian surface did not change and that backscatter can be highly dependent on the look direction.

Radar mapping was deliberately suspended again in mid-July in the hope that further rest might preserve enough transponder life to observe the last major gap in data coverage. The southern area from 315° to 330° longitude had eluded our efforts on three previous attempts. This area was missed right after orbit insertion when the "walkabouts" and "loss-of-signal" events occurred late in August 1990 and delayed the start of mapping by two weeks. Then, this area was missed again in May 1991, when we had to shorten the radar mapping periods to keep the spacecraft cool. Next, the transponder anomaly in Janu-

ary 1992 kept us from imaging this area for a third time. This area contains three large volcanoes (Ushas, Hathor, and Innini Montes) discovered by the Pioneer Venus Orbiter. Fortunately, after three misses, Magellan was allowed a "fourth swing" and the transponder rose to the occasion. An additional 2% of the planet was acquired during the first two weeks of September 1992. At that time, initial estimates placed the amount of cumulative mapping coverage at 99%. A more detailed analysis has revealed the actual coverage to be 98%. Total stereo coverage was 21%, an area equivalent to more than two-thirds of Earth's land area. Many thanks to the flight team, who brought us this success!

The time has come to give the radar a rest and set our sights on Magellan's other objective of understanding the structure and dynamics of the interior. Thus, the fourth mission cycle, from September 15, 1992, until May 25, 1993, is devoted to making gravity observations for 360 degrees of longitude. An Orbit Trim Maneuver (OTM) was performed on September 14, 1992, to improve these measurements. A 54-minute thruster burn slowed the spacecraft, allowing the gravity of Venus to pull Magellan's orbit closer to the planet. Periapsis, the point of the orbit closest to the surface, was lowered from 258 km to 184 km. The orbit period was shortened by 62 seconds, and periapsis will drift lower by 20 km over the duration of the cycle. The apoapsis (the highest point in the orbit) remains at 8,450 km. Cycle 4 will be extended to May 25 to repeat gravity measurements that were degraded by the passage of the radio signal through the Venusian atmosphere.

Gravity observations during Mission Cycle 4 are being conducted by observing minuscule changes in the spacecraft's velocity. The large high-gain antenna is pointed toward Earth instead of Venus during Magellan's orbit. Observations of the Doppler shift of the signal, with its high frequency (X-band, 3.6-cm wavelength), relatively high power, and large antenna, provide a measurement of spacecraft velocity. Variations as small as 0.1 mm/second can be detected. Spatially, a surface mass equivalent to a mountain 300 km in diameter and 1 km high nudges the spacecraft enough to be detected within 20 degrees of periapsis. Magellan's mapping of the gravity field for 360 degrees of longitude will help geophysicists understand the distribution of mass within the planet, along with processes that occur in the mantle. Additional comments about the gravity experiment are given in the accompanying article by Bill Sjogren, "Magellan Gravity."

The spacecraft is in good health. The batteries were reconditioned in September 1992, following the periapsis lowering maneuver, and the gyroscopes were calibrated in mid-November 1992. Also, the spacecraft has over 90 kg of hydrazine rocket fuel remaining (of the 120 kg that it had at launch).

The radar data from the first three mission cycles are now available, on various media and in various distribution modes, to the general public, educators, and the scientific community. Over 1100 radar mosaics are available at the National Space Science Data Center (NSSDC). More than 300 pictures have been publicly released, and several Magellan flyover videos are available. Also, the results of the radar mapping are contained in the August and October 1992 issues of the Journal of Geophysical Research (JGR) - Planets. These results are outlined by Steve Saunders in "Summary of Magellan Science Findings," in

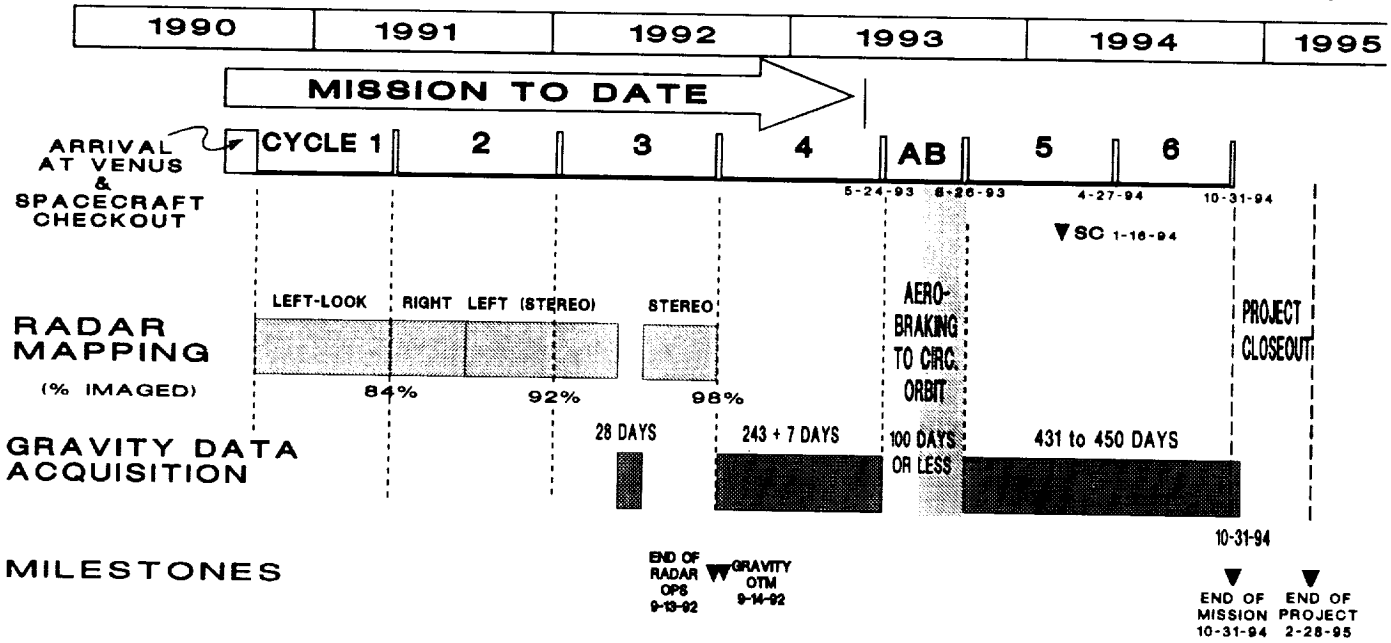

Figure 1. Magellan primary and extended mission plan.

this *V-Gram*.

Under the current plan, the Magellan mission will end within a few months after the conclusion of Cycle 4. The spacecraft will perform an aerobraking experiment in which periapsis will be again lowered, this time using the atmospheric drag to alter the orbit. If successful, the orbit will become more circular over 70 to 100 days without overheating critical spacecraft parts.

The resulting circular orbit would be useful for gathering high-resolution gravity data near the polar regions of Venus. But if additional operating funds are not available, Magellan will be abandoned in Venus orbit, mission operations will cease, and the project will officially end by the close of Fiscal Year 1993.

Unlike spinning spacecraft such as the Pioneer Venus Orbiter, which lasted for 14 years in Venus orbit, the Magellan spacecraft cannot survive for long without updates to its onboard computer systems. Overheating will probably destroy some critical subsystem, and the craft will go silent forever, eventually burning up in the dense atmosphere of Venus.

Magellan has far exceeded its mission and science objectives, and has demonstrated that low- to medium-cost planetary missions can be successful in providing us with important new information about our Solar System.

T.W. Thompson's biography appeared in the January 1989 V-Gram.

SUMMARY OF MAGELLAN SCIENCE FINDINGS

R. Stephen Saunders
Magellan Project Scientist

This article briefly summarizes some of the science findings of the Magellan mission. More complete discussions can be found in the August and October 1992 issues of the Journal of Geophysical Research (JGR) - Planets. The August issue's lead article (by R. Stephen Saunders et al.) summarizes the Magellan mission and the science findings. The Magellan mission's scientific objectives were to (1) provide a global characterization of land forms and tectonic features; (2) distinguish and understand impact processes; (3) define and explain erosion, deposition, and chemical processes; and (4) model the interior density distribution. All but the last objective, which requires new global gravity data, have been accomplished, or we have acquired the data necessary to accomplish them.

To meet these objectives, synthetic aperture radar (SAR) imaging and altimetry measurements were acquired over 98% of the planet. Several kinds of images were obtained in order to provide the best information for the interpretation of the landforms. During the first 243-day cycle (one Venus rotation), an incidence angle, or look-angle, profile was used that maximized the image coverage, resolution, and overall quality everywhere along the orbit. This profile caused the incidence angle to vary from about 15° near the polar regions to 45° at the equator. In the first cycle, we mapped 84% of Venus, more than meeting the mapping objectives. In the second mapping cycle, data collection was restricted in order to control spacecraft temperature. Much of the mapping was done at a constant incidence angle, and looking to the right (toward the west)—in the opposite direction from that of Cycle 1. In addition, in Cycle 2, some of the major gaps were filled with the same profile as was used in Cycle 1. In Cycle 2, we also conducted a successful test of a stereo mode in which the surface was viewed at a slightly different angle than that in Cycle 1. The stereo was so useful that we decided to devote much of the third mapping cycle to acquiring stereo images. All of the radar image data were processed at the Jet Propulsion Laboratory (JPL) in a complex flow that began at the Deep Space Network (DSN) stations at Goldstone, California; Madrid, Spain; and Canberra, Australia. Ray Piereson managed the JPL activity in the SAR Data Processing System and the Image Data Processing System. In addition to images and altimetry, we acquired radiometry data simultaneously with images. The radiometry is a measurement of the radio emission of the surface at the radar wavelength. This radio emission varies from place to place due to variations in surface properties (e.g., composition). Gordon Pettengill, head of the radar team, and Peter Ford accomplished the gargantuan task of processing all the altimetry and radiometry data.

Imaging was terminated at the end of the third cycle. Gravity data are being acquired during Cycle 4 by pointing Magellan's high-gain antenna at the Earth and recording changes in the radio signal's Doppler shift. From these changes, we extract the slight accelerations of the spacecraft as it orbits Venus. Gravity maps are then produced that provide information on density variations in the planet's interior. Because the antenna is pointed at the Earth, the acquisition of image and altimetry data is precluded.

One of the Magellan objectives was the acquisition of data for geodesy. Geodesy includes the determination of a planet's shape (originally that of the Earth), its gravity field, its rotation, and the position of its pole of rotation. With Magellan data, Mert Davies was able to determine the rotation period of Venus much more precisely than was previously known (243.0185 ± 0.0001 days). The north

pole is at right ascension 272.76° ± 0.02° and declination 67.16° ± 0.01°. The planet's mean radius is 6051.84 km, with the highest point being 6062.57 km and the lowest point 6048.0 km.

The basic framework for Venusian geology was compiled by the Pioneer Venus Team. The results of this mission were reported in 1980 by Hal Masursky and the rest of the Pioneer Venus radar team. In addition, scientists led by Valeri Barsukov and including Alexander Basilevsky analyzed Venera 15 and 16 image data. Their assessment, published in 1986, of the global importance of plains and highlands has been shown to be basically correct.

Venus can be subdivided simply into surfaces that appear to be mostly volcanic plains dotted with thousands of individual volcanic constructs and tectonically deformed highland plateaus. Volcanic plains, generally lowlands, make up about 85% of the planet. The remaining 15% are highlands, dominated by complex ridge terrains, sometimes referred to as tesserae. Duane Bindschadler has led the study of highland plateaus, which appear to be charac-

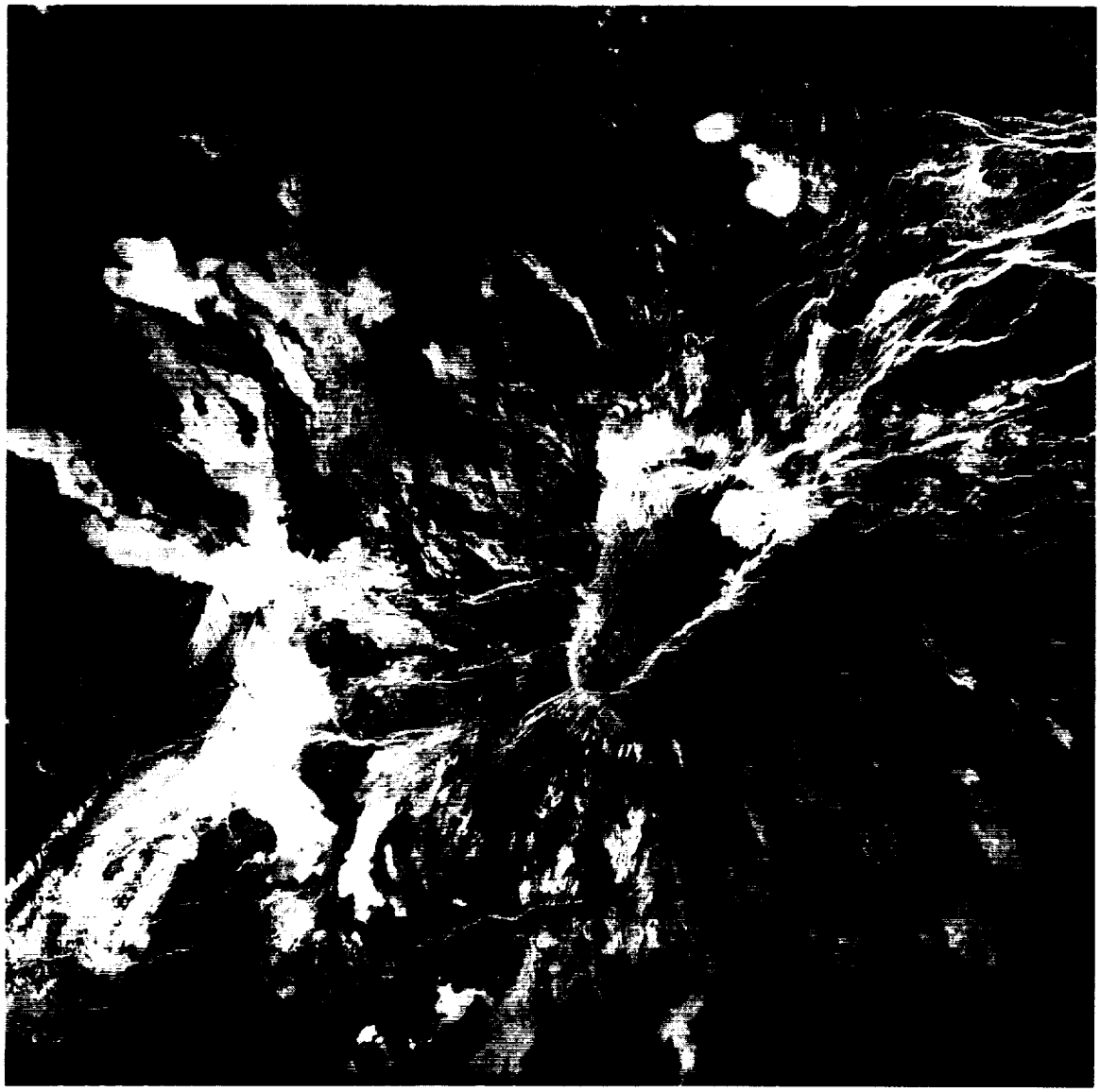

Figure 1. Located to the west of Phoebe Regio, this unnamed 2-km-high volcano is centered at 12.5°S latitude, 261°E longitude. It straddles a narrow fracture system that is probably extensional in origin. Lava flows radiate for distances of hundreds of kilometers from this volcano and appear both bright and dark to the radar, indicating a wide range of roughness at the radar wavelength scale of 12.6 cm. (P-40844)

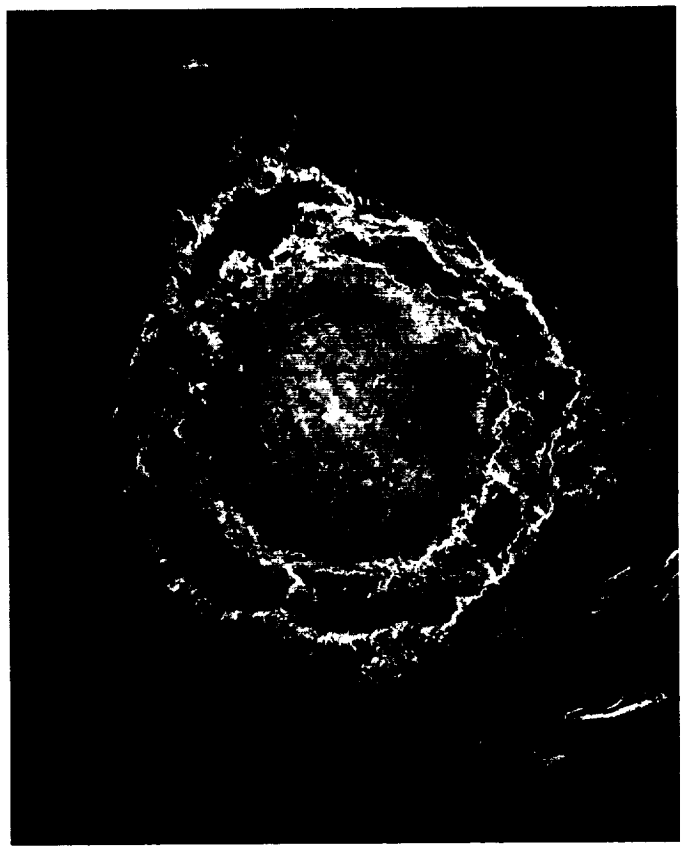

Figure 2. Mead Crater, the largest impact crater on Venus (280 km in diameter), is located at 12.5°N latitude and 57.2°E longitude. Mead—named after Margaret Mead, an American anthropologist (1901–1978)—is a multi-ring crater. Its innermost concentric scarp is interpreted to be the rim of the original crater cavity. The flat, somewhat brighter inner floor is interpreted to have formed from infilling of the original crater cavity by impact melt and/or by lavas. Emplacement of hummocky ejecta to the southeast of the crater rim appears to have been impeded by pre-existing ridges. (P-41461)

Figure 3. The crater Isabella, the second-largest impact crater on Venus (175 km in diameter), is located at 30°S latitude, 204°E longitude. This feature is named in honor of the 15th Century queen of Spain, Isabella of Castile. Two flow-like structures extend to the south and southeast. The end of the southern flow partially surrounds a pre-existing 40-km-diameter volcano. The southeastern flow contains a complex pattern of channels and flow lobes. Its tip is overlain by deposits from a later, 20-km-diameter impact crater, Cohn (named for Carola Cohn, an Australian artist, 1892–1964). (P-41056)

terized by compressional features. Examples are Western Ishtar Terra, Thetis Regio, and Phoebe Regio.

Volcanism dominates over tectonics and is the most widespread geologic phenomenon on Venus. Volcanic features are distributed globally over broad areas, unlike the linear distributions typical of the Earth. The most extensive volcanic units consist of very large flows called flood lavas. A variety of volcanic constructional features are seen. These include clusters of edifices, probably shield volcanoes, 10 km or less in diameter. Volcanic cones, smaller than shields, are also seen, and both are most likely basaltic in composition. Other constructional features include domes, which consist of lava with high apparent viscosity and which are thus probably of more silicic composition. Domes range in diameter from about 15 to 90 km and are typically circular and a few hundred meters in height. Scalloped domes are common and appear to have experienced slope failure on their flanks.

Ellen Stofan and Steve Squyres have studied coronae, a unique category of Venusian features which are classified as volcanotectonic. Coronae are surrounded by a ring of tectonic features ranging from extensional to compressional and have variable topography. The distribution of coronae is not random: they are concentrated in a few groups and along several chains. Coronae share many morphologic characteristics with volcanic rises; their morphology suggests that coronae resulted from either smaller mantle plumes or shorter lived mantle plumes than those associated with volcanic rises. Crosscutting relationships at several coronae suggest that formation of radial troughs precedes formation of concentric ridges and troughs. This suggests a genetic link between radially fractured domes (coronae dominated by radial troughs) and coronae dominated by concentric graben, which may indicate different stages in corona evolution. Similarities between radially fractured domes and shield volcanoes also suggest a genetic relationship.

Jim Head and his students and associates have catalogued more than 1660 volcanic land forms, related features, and volcanic deposits. These include over 550 shield fields; 274 intermediate volcanoes 20 to 100 km in diameter; 156 large volcanoes greater than 100 km in diameter; 86 caldera-like structures, not including those associated with shield volcanoes; 175 coronae; 259 arachnoids (defined as having inner concentric and outer radial ridges and fractures); 50 novae (radial-fracture features); 53 lava flow fields; and 50 sinuous lava channels. Of these features, 145 steep-sided domes have morphologies similar to those of terrestrial domes that formed by viscous, andesitic, dacitic, and rhyolitic lavas. Studies of these domes by Betina Pavri suggest that they are located in areas in which their source of magma has undergone extensive evolution. A large number of steep-sided domes, the so-called pancake domes, are almost perfectly circular in map view. Magellan images for the region of the Venera 8 landing site indicate that the lander is located in mottled plains, a stratigraphically younger plains complex, and near a steep-sided dome and a caldera. It had previously been determined that the site was one of two Venera landing sites with nontholeiitic compositions. Alexander Basilevsky has suggested that these may be regions of more evolved crust, like the granitic cores of Earth's continents. Dan McKenzie has postulated that the similarity between the shape of seven large steep-sided "pancake domes" and that of a theoretical model of an axisymmetric gravity current spreading over a rigid horizontal surface suggests that the domes were formed by a fluid with a simple viscous flow behavior.

Some of the larger volcanoes, such as Sif Mons and Gula Mons in Western Eistla Regio, occupy regional topographic rises. Dave Senske has been studying this region using Arecibo images, and now, with Magellan data, he has led an effort to summarize the studies and mapping of this area. Dave and his co-authors conclude that mantle upwellings may create the topographic rise areas such as Beta Regio.

Another type of large-scale volcanic phenomenon, studied by Kari Roberts, is large flow fields such as Mylitta Fluctus. This feature, located in Lavinia Planitia, was first identified in Arecibo images. With Magellan data, Kari was able to compile detailed maps of the features associated with this massive lava flow field.

Vic Baker has led the examination of sinuous channel features that are found on the plains of Venus. He and his team have mapped about 200 channel and valley land form complexes. Channel types include (1) simple channels, such as sinuous rilles, canali, and channels with high width-to-depth ratios, (2) complex channels, and (3) compound channels. Channels are globally distributed with the large, canali type occurring in the plains. Some channels, where they cross ridges, have streamlined hills and spill relationships that are similar to features in terrestrial flood channels. A variety of lava types have been proposed to be associated with channels. Among these types are fluids from ultramafic silicate melts, sulfur, and carbonate lavas. Each of these lava types would have different, but profound, implications for Venusian geology. The channels have extreme longitudinal uniformity. If they formed by flowing liquid, then the surfaces on which they flowed were uniform and nearly level, approaching an equipotential surface. Longitudinal profiles of most channels vary in elevation by hundreds of meters along the channels, indicating postchannel deformation of the plains surface.

Lava flows on Venus have a wide range of radar reflectivity, from very dark, smooth surfaces to bright,

Figure 4. A 200-km-long segment of a sinuous channel, approximately 2 km wide, is shown in this image centered at 9°S latitude, 273°E longitude. Channel features like this appear to have been formed by lava that may have melted or thermally eroded a path over the surface. These features resemble terrestrial rivers in many respects, with meanders, cutoff oxbows, and abandoned channel segments. Many are partly buried by younger lava plains, making their sources difficult to identify. Cross-cutting relationships show that this feature postdates an earlier channel and is itself crossed by fractures and wrinkle ridges, indicating that it is relatively old. In addition, it runs both upslope and downslope, suggesting that the plains were warped by regional tectonism after the channel formed. (P-39226)

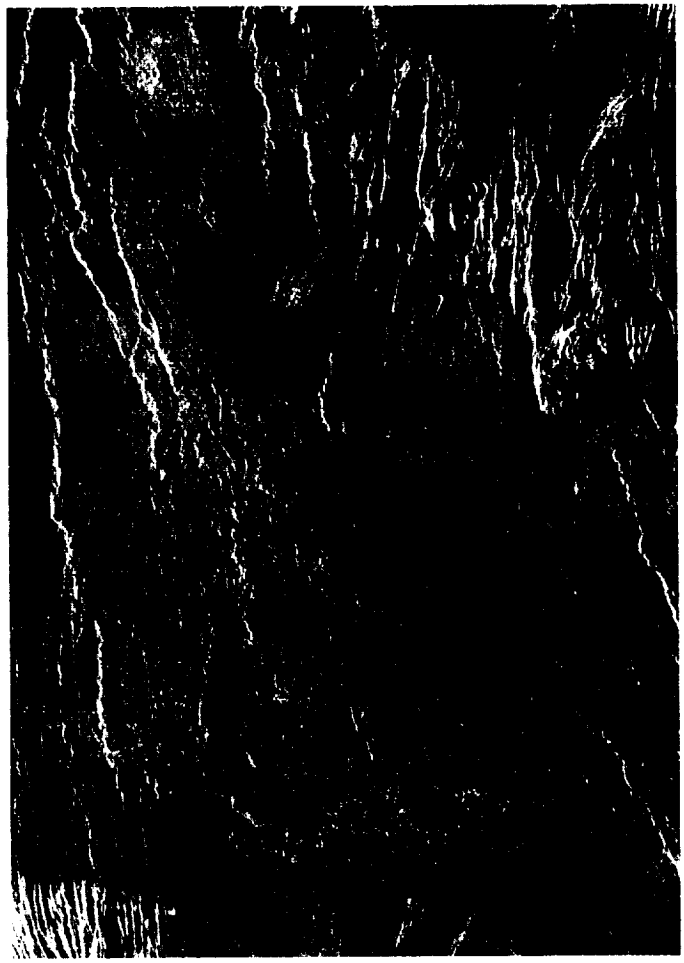

Figure 5. Lying along a north-south trend and centered at 28°N latitude, 283°E longitude is the 1050-km-long rift valley Devana Chasma, in Beta Regio. The rift is similar to areas on the Earth such as the East African Rift where the crust is being stretched and faulted. Devana is 240 km at its widest point and narrows to a width of 80 km where it intersects a region of tesserae to the north. Rhea Mons is located near the top center of the image and is distinguished by a radar-dark oval area at its summit. To the south of Rhea, the 37-km-diameter "split" impact crater Somerville has a rim that has been extended and separated by a distance of about 10 km. (P-41294)

rough surfaces. Bruce Campbell and Don Campbell have examined the radar properties of Venusian lava flows and compared them with those of terrestrial flows. Scattering from lava flows in Eistla Regio, Northern Sedna Planitia, and Southern Lavinia Planitia is less than that of terrestrial pahoehoe lavas. Only the most radar-bright areas equal or exceed the radar-brightness of terrestrial a'a. These Venusian volcanic deposits have typical dielectric constants of 3 to 5, which are in the range of low values for terrestrial basaltic flows. This suggests that the volcanic deposits in these areas are similar to terrestrial pahoehoe and transitional flows, whereas a'a flows are uncommon or absent.

Sean Solomon organized the study of tectonic features using Magellan data. Magellan mapping has revealed deformational features of a wide variety of styles and spatial scales ranging from several kilometers to thousands of kilometers. Deformation is manifested both in widely distributed strain of modest magnitude and in areas of concentrated extension and shortening. Several regions show evidence of lateral extension and collapse during and following crustal compression. Extension is expressed in two forms: quasi-circular coronae and broad rises with linear rift zones. Evidence for horizontal displacements suggests that extensional deformation may be limited to a few tens of kilometers (e.g., a split crater in Devana Chasma). There appear to be a few large offset strike-slip faults, but more commonly, there is limited local horizontal shear across zones of crustal shortening. The presence of slopes in excess of 20° to 30° over scales of tens of kilometers indicates active tectonics. Deformation is distributed across broad zones on Venus, unlike on the Earth, which has narrow zones of deformation at rigid plate boundaries. Craters and other geologic features have been disrupted by tectonic activity, indicating that Venus has been tectonically active during recent epochs.

Sue Smrekar conducted an extensive study of Western Ishtar Terra, a region that contains an abundance of tectonic features. Troughs and lineations interpreted to be graben and normal faults trend perpendicular to topographic slopes in the mountain belts and plateau margins of Ishtar Terra. This suggests that the graben sets formed as a result of gravitational spreading. Models estimating rates for extensional failure and topographic relaxation indicate that the crust of Western Ishtar Terra is much stronger than that predicted by flow laws. Alternatively, the relief and high slopes may have been actively built and maintained until recently in comparison to the mean Venusian surface age of 500 million years (m.y.), that is, within the past few tens of million years or less, rather than the past few hundred million years.

Robbie Herrick and Roger Phillips have concluded that the correlation of large shield volcanoes with geoid anomalies suggests evidence for large-scale mantle upwelling, with downwelling possibly occurring in the plains. No specific correlations with gravity models are found for coronae. Smaller geoid to topographic ratios correlate well with highland tessera regions, which suggests crustal compensation and areas of thickened crust. The lack of hot-spot tracks does not support Earth-like plate-tectonics for Venus.

One of the more surprising observations has been made by Dan McKenzie. Although no evidence for Earth-style plate tectonics has been found on Venus, features associated with some coronae and arcuate trenches in the Dali-Diana trough system have morphology that resembles terrestrial subduction trenches.

Dave Sandwell and Jerry Schubert have examined structural models that might apply to large coronae. The trench and outer rise morphology around major coronae suggests that the lithosphere is flexed downward, possibly by loading or as a consequence of a surrounding passive lithosphere that is subducting and rolling back underneath an expanding corona. From analysis of these features, elastic thicknesses and bending moments were determined with values similar to those of terrestrial trenches (e.g., the Mariana, Middle America, and Aleutian trenches).

Duane Bindschadler led the effort to study the complex ridge terrains (CRTs), sometimes called tesserae. The morphology of tectonic features comprising CRT in Alpha Regio and the stratigraphic relationships they reveal support a mantle downwelling model better than a hot-spot model for CRT formation. Linear deformation zones (LDZs) in the Alpha Regio CRT are interpreted to be shear zones. Small graben in Alpha are believed to have formed from gravitational relaxation of the highlands in the latest stage of CRT development. Jerry Schaber headed the group that studied the Venusian impact craters. Impact craters provide important clues to the geologic evolution of planetary surfaces, since such craters form randomly in time and space. Unfortunately, there are too few impact craters on Venus to estimate surface ages other than on a global scale. The slow rate of surface modification processes on Venus is evidenced by the fact that most Venusian impact craters appear unmodified by weathering processes. Crater diameters range from 2 to 275 km, though at small diameters, less than 35 km, there is a deficiency of craters because of the atmosphere's shielding effect. The analysis reported to date lists 912 craters observed on 98% of Venus. The estimated surface age is between 200 and 700 m.y. Schaber has argued that the crater evidence indicates a period of catastrophic resurfacing by volcanism and relatively little volcanic activity since. As on other cratered surfaces in the solar system, Venus has a progression of crater morphologies with increasing diameter from flat-

Figure 6. This Magellan image shows a portion of Leda Planitia, centered at 41°N latitude, 52°E longitude and covering an area 220 km wide and 275 km long. Several examples of major geologic terrains are illustrated, along with a basic stratigraphy or sequence of geologic events. The oldest terrains, seen in the upper left of the image, are radar-bright highly fractured or chaotic highlands that rise above the plains. These uplands, called tesserae, occupy about 15% of the surface of the planet and may represent thicker crustal material. The circular ring structure in the lower left of the image is a 40-km-diameter impact crater named Heloise, after the French physician (1098–1164). Both the crater and the tesserae are embayed, predating the emplacement of plains lavas that covered the region. The most recent activity is volcanism that produced the radar-bright flows seen in the lower right and upper right part of the image. The geologic history of this area is characterized by: (1) early fracturing and formation of the tesserae and impact crater; (2) lava flooding, forming extensive dark plains; and (3) emplacement of bright, less extensive flows on the plains surface. (P-39659)

floored, central peak, peak ring to multi-ring craters. Craters smaller than 30 km are commonly irregular due to multiple strikes from disrupted projectiles. The percentage of craters with radar-bright volcanic-appearing outflows increases with increasing crater diameter. Bright outflows appear to have been created by a low-viscosity fluid which may be likened to pyroclastic flows from volcanoes on Earth. Bright and dark "splotches," typically about 20 km in diameter, are shock wave signatures of asteroidal bodies that did not survive the passage through the atmosphere.

Roger Phillips took an independent look at impact craters and related phenomena. From the number of impact craters, he and his colleagues deduced a production age, or mean surface age, of about 500 m.y. Their analysis supports either catastrophic global volcanic resurfacing some 500 m.y. ago, or smaller scale equilibrium resurfacing occurring in small events spread over time, covering approximately 1 km^2/year. Statistical analysis of the crater distribution shows that it cannot be distinguished from a completely random distribution on the sphere. Studies by Phillips and his colleagues show that the smallest craters whose numbers are not affected by the atmosphere are 30 km in diameter. It is observed that there may be a lower crater density near those craters that are partly filled by volcanic material. This suggests that some craters have been completely covered.

The atmosphere of Venus has a profound effect on all aspects of impact cratering. Pete Schultz has found that craterless radar-bright scour zones (splotches) are the result of atmospheric cratering. This is where energy is transferred from the impacting object to the atmosphere directly prior to impact or indirectly after impact through deceleration of ejecta and impact-generated vapor. The maximum diameter for an impactor undergoing this type of failure is 3 to 4 km. Run-out flows, or outflows, extend to about a crater radius from the rim before following local slopes as low as 0.03°. The outflows are seen as thin turbidity flows, which may indicate volatile-rich impactors (25% of the crater population) and laminar flows, which may indicate silicate or iron-rich impactors (58%). Others are composite flows. High-resolution images of well-preserved impact crater morphologies reveal stages of impact crater formation in the following order: (1) atmospheric cratering which creates the splotch; (2) indirect transfer of kinetic energy to the atmosphere before excavation, forming radar-bright halos and downrange rim depressions; (3) formation of run-out flows; (4) emplacement of ejecta, including pressure-differential scouring and redirected ejecta flows by recovery winds; and (5) late-stage fallout from recondensed vapor, forming radar-dark parabolas. Crater scaling relations are controlled by atmospheric pressure rather than gravity, and a reduction in cratering efficiency may result in smaller crater diameters and underestimation of the surface age.

A significant crater-related phenomenon is the large parabolic halos associated with many impact craters. The parabolas can be bright or dark and are always open to the west, with the crater near the focus. Don Campbell studied these features and found 54 parabolic-shaped and 9 approximately circular large surficial impact-crater–related features in Magellan SAR images and emissivity data. All the parabolic features (with six exceptions) are oriented E-W, with the apex at the east end. Sizes of these features range from several hundred to 2000 km, and the dimensions are loosely correlated with the size of the impact craters. About one-third of all craters > 15 km in diameter have bright floors, and half of these have parabolic features (note that almost all craters with parabolas have basins with high reflectivity and low emissivity). No features have been found overlying the parabolas, indicating that they are among the youngest features on the surface of the planet. This suggests that radar-bright craters may be young and unmodified. The observed patterns and geologic associations are consistent with a model of small particles injected into the upper atmosphere at the time of impact and carried to the west by the E-W zonal winds. The size of the individual particles can be as large as 1 to 2 cm; the deposit depth is a few centimeters to a few meters.

A somewhat unexpected finding in the Magellan images was an abundance of wind streaks. These features have been mapped and classified by Ron Greeley. There is widespread evidence of eolian activity; more than 8000 wind streaks have been identified. Most streaks are seen between 17° and 30° south latitude, and 5° to 53° north on smooth plains. Streaks are usually associated with deposits from nearby impact craters and with debris within some tectonically deformed terrains. Wind streaks are generally oriented with the downwind direction toward the equator, consistent with the Hadley model of atmospheric circulation. Other eolian features discovered include dune fields and possibly yardangs.

Ray Arvidson conducted a broad study of Venusian surface processes. Arvidson and the members of his team found evidence for weathering, mass wasting, and eolian activity operating on a continuous basis. Stratigraphically young flows in Sedna Planitia have radar signatures similar to those of terrestrial a'a and pahoehoe flows; older flows have backscatter characteristics akin to those of terrestrial flows degraded by weathering or buried by eolian deposits. The parabolic crater deposits, made up of fine debris distributed by high-speed zonal E-W winds, are determined from their microwave properties to be centimeters thick. High radar reflectivity in most of the highlands suggests an elevation-dependent surface-atmospheric in-

teraction. Evidence in Western Ova Regio indicates that this alteration occurs at a lower rate than mass wasting and eolian activities. The average plains resurfacing rate by surface processes is on the order of 10^{-2} μm/year. This is comparable to rock erosion rates on Mars.

Gordon Pettengill and Peter Ford have worked with the radiometry data and confirmed their previous findings for the presence of areas of extremely low values of radiothermal emissivity. Some values are as low as 0.3. The global mean value of emissivity is 0.845, corresponding to a dielectric permittivity of 5.1, a value consistent with dry basaltic surface material. Possible explanations for anomalously low values of emissivity are (1) an interaction at the interface between the atmosphere and a high-dielectric permittivity medium such as metal-bearing mineral deposits, or (2) multiple scattering from within the volume of a very low loss, near-surface medium containing many sharp discontinuities. Smaller variations in emissivity (over the interval from 0.8 to 0.9) may be due to differences in surface roughness, density of the material, or composition.

Mike Malin has identified rock slumps, rock or block slides, rock avalanches, debris avalanches, and debris flows (there is little evidence for regolith and sediment movements) in areas of high relief and steep slopes. The features are most common in troughs or graben. Venusian landslides typically come from escarpments higher than those on Earth; they are larger than terrestrial subareal landslides but smaller than Martian ones. Oversteepening

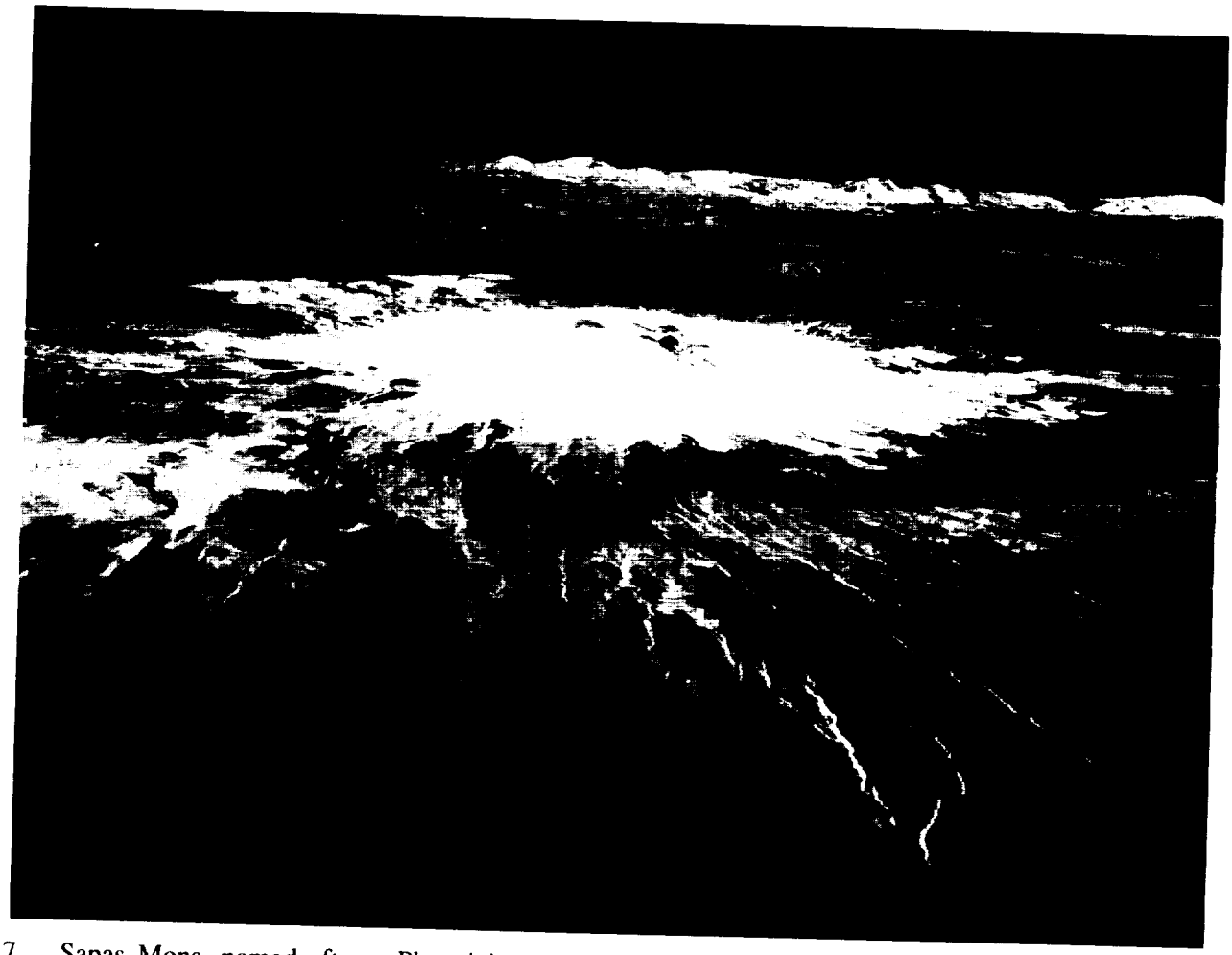

Figure 7. Sapas Mons, named after a Phoenician goddess, is displayed in this computer-generated perspective. Magellan SAR data are combined with radar altimetry to develop a three-dimensional map of the surface. The view is to the north, with the volcano at the center of the image, located at approximately 0.9°N latitude, 188°E longitude. Sapas rises 3 km above the mean surface, with radar-bright lava flows extending for hundreds of kilometers into dark, smooth plains. Many of the flows appear to have erupted from sources on the flanks of the volcano rather than from the summit. Flank eruptions are common at large volcanoes on Earth, such as in Hawaii. The topographic relief is exaggerated approximately 10 times. (P-40701)

by intrusion and subsequent lateral collapse occurs on some large volcanoes (in particular, scalloped domes).

Jeff Plaut and Ray Arvidson have compared Magellan and Goldstone images of features in the equatorial plains. Both Magellan and Goldstone data show high dielectric constants on impact-related parabolic surfaces. Comparison of Magellan SAR data with rough surface scattering models and SAR data of terrestrial surfaces indicates that the roughness characteristics of the equatorial plains are comparable to those of modified terrestrial lava flows.

Areas with unusually high dielectric constants occur at high elevations above a threshold elevation that varies from 4.75 km above the mean planetary radius at Maxwell Montes to < 0.6 km. Brennan Klose believes that the absence of highly reflective material at the 8-km-high summit of Maat Mons suggests the lavas have not had sufficient time to weather and thus may have been recently emplaced.

Len Tyler led a group that determined backscatter functions from the Magellan image and altimetry data. Empirically derived backscatter functions for incidence angles less than 4° to 10° have been derived from Magellan altimetry radar echoes. Root mean square (RMS) slopes can be derived with these functions.

It is not possible to name all the hundreds of people who contributed to these preliminary interpretations. I have tended to identify first authors, but we should recognize that many co-authors and associates contributed to the work in countless discussions and with generous sharing of ideas and hard work.

References

Journal of Geophysical Research, Volume 97, Number E8, August 25, 1992, and Volume 97, Number E10, October 25, 1992.

R.S. Saunders' biography appeared in the October 1986 V-Gram.

EXCERPT FROM "ACQUISITION AND ANALYSIS OF MAGELLAN GRAVITY DATA" (FROM *V-GRAM 14*)

M. Ananda, G. Balmino, N. Borderies, M. Lefebvre, B. Moynot, W. Sjogren, and N. Vales

Introduction

Gravity data, as discussed here, are measurements of small variations from the total acceleration acting on an orbiting spacecraft. When a spacecraft is relatively close to a massive body like Venus, it experiences nonuniform accelerations due to surface irregularities and/or density variations within the planet. Speed variations can be determined by precisely measuring the speed of the spacecraft every few seconds with an Earth-based radio tracking system. These changes in speed are accelerations, or gravity measurements. Their peak amplitudes are less than 1 mm/second^2 (100 milligals). The raw-speed measurement, made between the Earth-based antenna and the orbiting spacecraft, contains many large motions which must be removed a priori before gravity field signatures can be extracted. These motions include: the rotation of the Earth (400 m/second), the relative motion of the Earth with respect to Venus (30 km/second), and the primary orbital motion of the spacecraft around Venus (8.2 km/second). Additional factors that must be considered are signal transit times, effects of the Earth's troposphere and ionosphere, solar radiation, solar- and planetary-body perturbations, and relativistic effects.

The closer the spacecraft is to the surface of the planet, the better will be the Doppler data sensitivity to mass variations. A rough rule of thumb is that the feature resolution will be approximately equal to the spacecraft altitude. Therefore, the smallest detectable gravity feature that Magellan will resolve will be about 200 to 250 km.

Doppler Data System

The acquisition of gravity data is accomplished via the Deep Space Network Tracking System, which uses the radio antennae located at Goldstone, California; Madrid, Spain; and Canberra, Australia. The system also uses the transponder onboard the Magellan spacecraft. A radio signal is transmitted from the Earth, is received at the spacecraft's transponder, and is then retransmitted to the antenna on Earth. The received signal is differenced with the very stable signal that was initially transmitted; the difference represents the Doppler data that are used for gravity field analysis. JPL's Navigation Team uses the same data to estimate the spacecraft's orbital position. It is the fine structure left in the Doppler residuals, once the a priori motions and estimated spacecraft orbital motion have been removed, that provides the information for gravity field estimation.

The heart of the system is composed of the very stable oscillators at the tracking station sites. The oscillators are hydrogen masers that are accurate to better than 1 part in 10^{13} over the integration times. This stability allows the extraction of gravity measurements to approximately the 1-milligal level (.01 mm/second^2) at the spacecraft altitude. Another important feature of the Magellan system is the use of the X-band uplink frequency (8.3×10^9 cycles per second), which is significantly less sensitive to the

corruptive effects of space plasma than was the old S-band system.

Biographies for M. Ananda, G. Balmino, N. Borderies, M. Lefebvre, B. Moynot, W. Sjogren, and N. Vales appeared in the March 1986 V-Gram.

MAGELLAN GRAVITY

William Sjogren
Magellan Gravity Investigation Team,
Principal Investigator

The gravity investigators and geophysicists on the Magellan project obtained their first high-resolution data set after waiting patiently for over two years. On September 14, 1992, the periapsis altitude of the Magellan spacecraft was lowered to 182.5 km. Doppler gravity data through periapsis are being acquired continuously until May 25, 1993, when 360 degrees of longitude coverage will be completed.

The reason for this long delay was partially explained in *V-Gram 14*, but the primary change to that original schedule has been the need to maximize the SAR imaging data before there was a failure in the complex SAR imaging system. In hindsight, it appears that the project took the correct action, for indeed the telecommunication system for sending the data was very near complete failure by the end of Cycle 3. When SAR data are acquired, the high-gain antenna is pointed toward Venus and precludes the acquisition of high-resolution gravity data.

Just prior to periapsis occultation in Cycle 3 (April 22–May 11, 1992), X-Band Doppler data through periapsis were acquired during 16 orbits. These data provide only a very limited sample of gravity coverage, but they do allow us to evaluate and compare the data quality with previous S-Band data coverage from the Pioneer Venus Orbiter (PVO) over this same region of Venus. The top half of Figure 1 shows the Doppler residuals from PVO's S-Band system, while Doppler residuals from Magellan's X-Band system are displayed in the bottom half. The systematic signatures are due to gravitational effects. Both residual plots are at the same vertical and horizontal scales and over approximately the same terrain. It is obvious that the Magellan data are far less noisy than the PVO data (by a factor of 10) and reveal subtler systematic effects. The PVO data have larger amplitude signatures because the PVO spacecraft was 100 km lower than Magellan and was therefore perturbed much more by the planet's lateral mass distribution. Even so, the small-scale anomalies in the Magellan data are easily detected, whereas in the PVO data, they are lost in the noise. Since Magellan has now lowered its periapsis altitude, its Doppler data amplitudes are comparable to those of PVO. Magellan altitudes are now lower than PVO's in the higher latitudes due to an orbit eccentricity of 0.39 versus one of 0.84 for PVO. Thus Magellan will be providing larger amplitude signatures as well as much higher quality data.

However, because Magellan's orbit is eccentric, the gravity resolution is not uniform and is seriously degraded in the high latitudes due to high altitudes. Figure 2 provides a comparison of Magellan's eccentric orbit versus a near-circular orbit which would provide uniform resolution. It is the ultimate desire of the gravity investigators and their colleagues in the geophysics community to attain this near-circular orbit, so all detectable features on Venus can be resolved uniformly. Therefore, it is proposed that after May 25, 1993, the project start an aerobraking sequence that will subsequently place Magellan in a near-circular orbit.

A study was performed to reveal the strength of this circular geometry. Theoretical Doppler data were calculated for the eccentric and the near-circular orbits both passing over the same Venusian terrain. The terrain be-

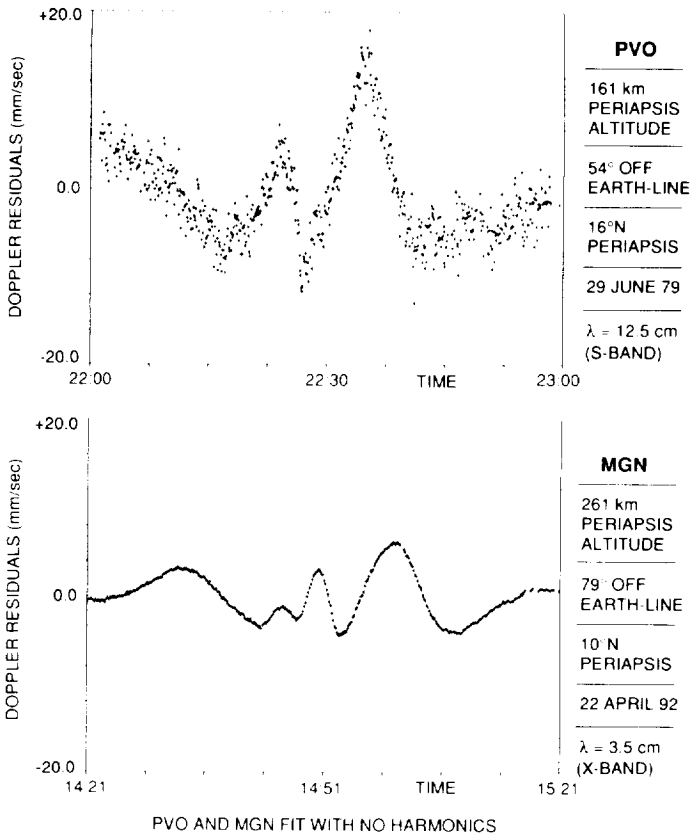

Figure 1. PVO and Magellan gravity data at same longitude.

neath the orbital track was composed of 25 surfaces masses (positive and negative) located between 90° north latitude and 90° south latitude. After reduction of the theoretical Doppler data, the detection of the gravity anomalies for each orbit was plotted. This is shown in Figure 3: the detection of high-latitude (beyond + 50°) anomalies is essentially nonexistent using the eccentric orbit's data, but all anomalies are easily determined by the near-circular orbit's data.

The data set after aerobraking will allow detailed analysis of similar types of features and their behavior globally as well as regionally. Coronae and large craters should be detectable. Spherical harmonic coefficients to degree and order of at least 75 will be derived, providing a global spatial resolution of approximately 250 km. Maxwell Montes, the largest topographic relief, will be clearly resolved, as will other features in the polar regions.

W. Sjogren's biography appeared in the March 1986 V-Gram.

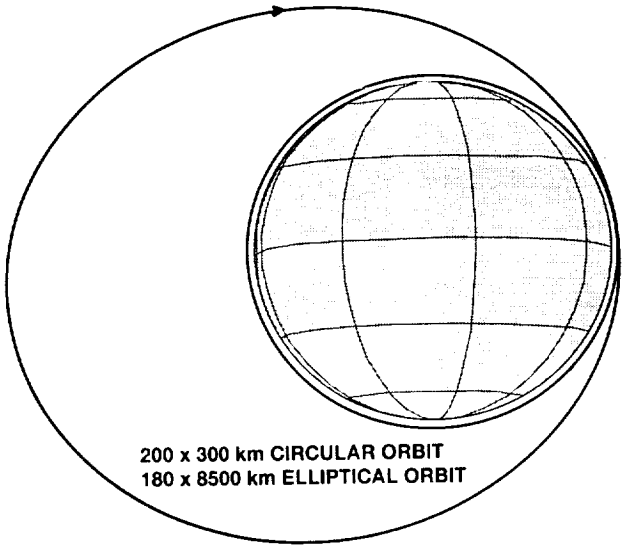

Figure 2. Circular and elliptical Magellan gravity orbits.

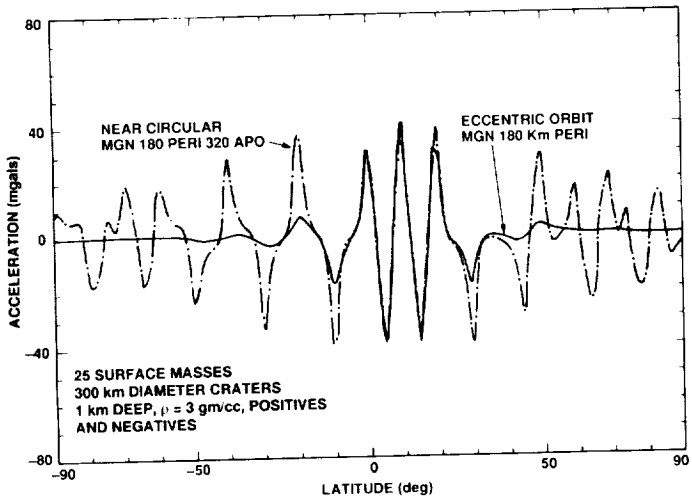

Figure 3. Gravity anomaly detection.

MAGELLAN STEREO IMAGE DATA

Jeffrey J. Plaut
Research Associate, Magellan Science Team, Jet Propulsion Laboratory

Introduction

Topographic features in radar images are always distorted to some degree. The amount of distortion depends on the topographic relief and on the incidence angle of the observation. During Magellan's extended mission (Cycles 2 and 3), a different viewing geometry was used than in Cycle 1, providing the opportunity to derive heights and depths of features at a lateral resolution comparable to that of the synthetic aperture radar (SAR) images. This article presents the mechanics of radar "stereo" imaging, along with a description of the Magellan stereo data set and examples applying the techniques to Magellan images.

Radar Image Distortion—Why Stereo Works

The location of a resolution cell in a radar image is determined across-track by the range (distance) between the antenna and the feature (measured as a time delay of the echo), and along-track by the Doppler shift expected for a given piece of terrain. The range-Doppler coordinate of a resolution cell can be easily transformed into planetary coordinates (i.e., latitude and longitude), under an assumption of the large-scale shape of the surface. In the case of Magellan data, the large-scale shape of the surface (at scales of hundreds of kilometers) is modeled as gently sloping (the "topo model") or as a portion of a perfect planetary sphere.

The use of the range coordinate leads to distortion of topographic features. For example, high areas will return an echo sooner than will the surroundings, and thus will be displaced toward the spacecraft in the image plane. The opposite is true for low areas. These are the effects known as "foreshortening" and "elongation." In the extreme case of foreshortening, an echo is received from the top of a mountain before the echo from the near-range base of the mountain, leading to "layover." Foreshortening and elongation can often complicate analyses of radar images, but

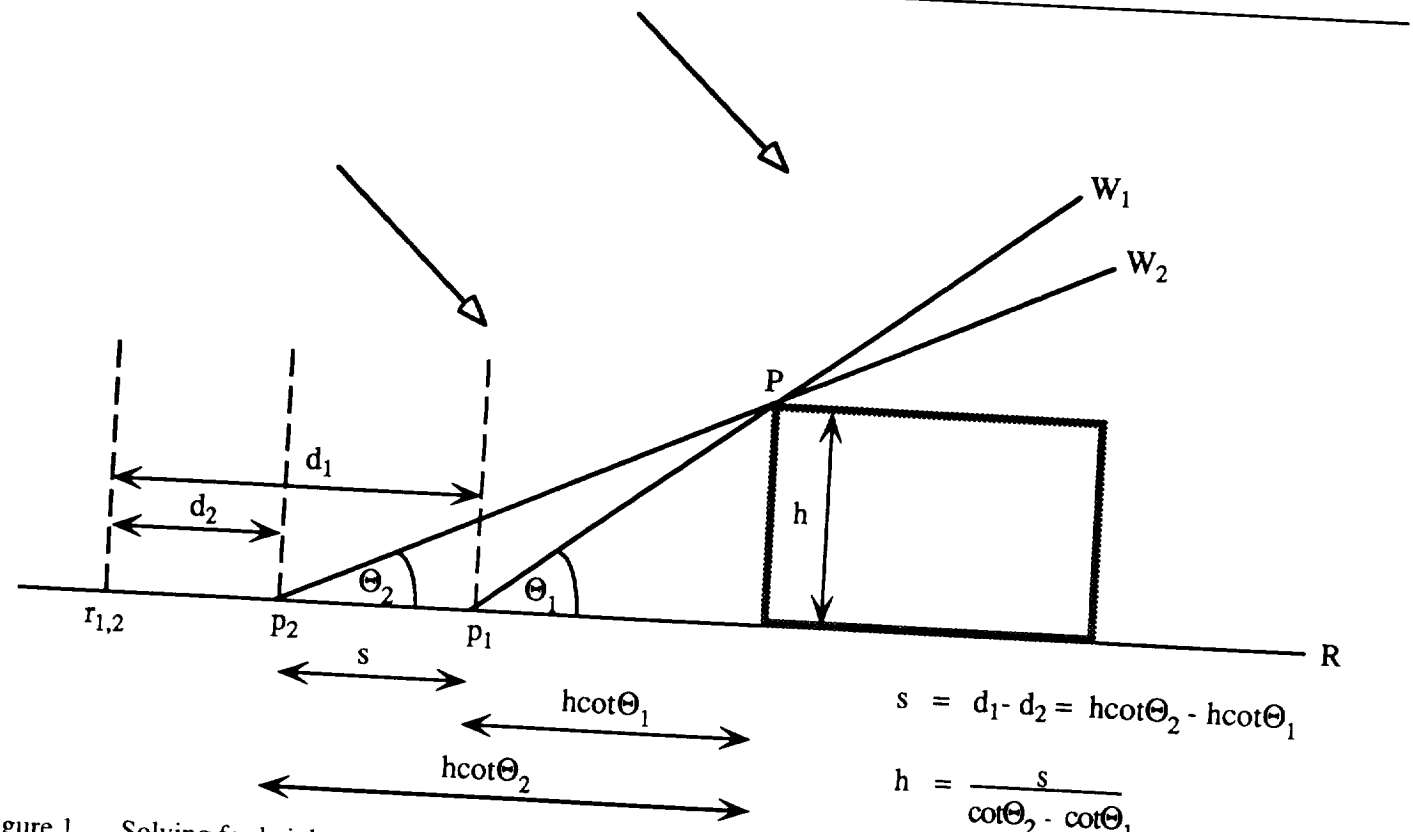

Figure 1. Solving for heights using same-side stereo images. The problem is to determine the height of point P above the reference plane, R, using measurements from the stereo image pair. As wavefront W_1 intercepts point P, the projection in range space (i.e., time delay) places the echo from P at point p_1 on plane R. Similarly, in the second image, the echo from point P is placed at point p_2. Identify a point $r_{1,2}$ on the plane R and measure the distance from $r_{1,2}$ to p_1 on image 1, and from $r_{1,2}$ to p_2 on image 2. The difference of these distances (d_1 - d_2) is s, the parallax of point P. Using the incidence angles of the two observations (Θ_1 and Θ_2), the height of the feature, h, is obtained by dividing s by the parallax-to-height ratio ($\cot\Theta_2$ - $\cot\Theta_1$).

they also allow us to determine heights of features with stereo techniques.

The amount of distortion is a simple function of the height of the feature and the incidence angle of the observation (Figure 1). Smaller incidence angles will produce greater distortion for a given amount of topographic relief. Thus, by comparing the distortion on two images taken at different incidence angles, a solution of the heights of features can be obtained.

Terrain relief can also be perceived visually, using same-side stereo pairs and a stereoscope. The larger incidence angle image (Cycle 1) should be viewed with the left eye, and the smaller incidence angle image (Cycle 3) with the right eye. Most people find opposite-side stereo image pairs difficult to fuse with a stereoscope.

Estimating Heights From Stereo Data

Feature heights may be obtained from same-side stereo image pairs (Figure 1), such as those from Magellan Cycles 1 and 3, and from opposite-side stereo image pairs (Figure 2), such as those from Magellan Cycles 1 and 2, or 2 and 3. In either case, an accurate measurement can be made only if the two points for which a height difference is to be found can be identified unambiguously in both images. Errors in identification of the features will be propagated as errors in the height determination. The appearance of features is often more similar in same-side image pairs than in opposite-side image pairs, making the height determination easier in the same-side case.

Stereo measurements are best made from high-resolution digital data (e.g., Magellan full-resolution mosaics), in which the precise pixel location of features can be made on a video monitor. Hard-copy prints may also be used, but the image pair must be enlarged to a single scale. Once the separation of the two features has been measured on the images and converted to a ground distance, the height difference is easily calculated, using the parallax-to-height ratio. The incidence angles of the two observations can be obtained from the ancillary files on Magellan CD-ROMs.

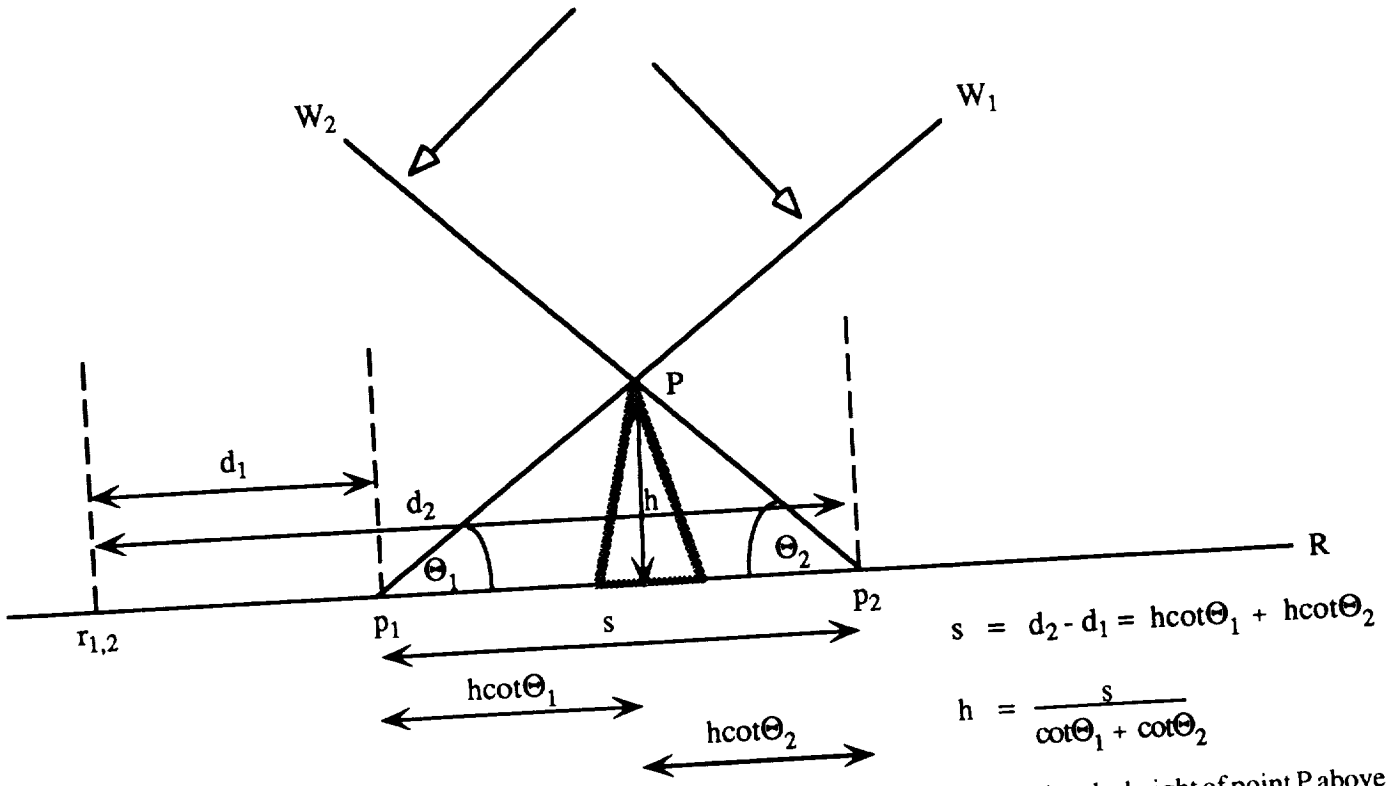

Figure 2. Solving for heights using opposite-side stereo images. The problem is to determine the height of point P above the reference plane, R, using measurements from the opposite-side stereo image pair. As wavefront W_1 intercepts point P, the projection in range space (i.e., time delay) places the echo from P at point p_1 on plane R. Similarly, in the second image, the echo from point P is placed at point p_2. Identify a point $r_{1,2}$ on the plane R and measure the distance from $r_{1,2}$ to p_1 on image 1, and from $r_{1,2}$ to p_2 on image 2. The difference of these distances ($d_2 - d_1$) is s, the parallax of point P. Using the incidence angles of the two observations (Θ_1 and Θ_2), the height of the feature, h, is obtained by dividing s by the parallax-to-height ratio ($\cot\Theta_1 + \cot\Theta_2$).

Note that the parallax-to-height ratio is obtained with a different formula for same- and opposite-side stereo pairs (Figures 1 and 2).

Magellan Stereo Data

Magellan Cycle 1 data were obtained in a left-looking, variable incidence angle mode. To maximize image quality and resolution, incidence angles were kept as large as possible. In Cycle 2 a right-looking mode was used, in which the incidence angle was kept constant at about 25° for most of each orbit. Incidence angles in Cycle 3 were selected to provide same-side stereo images complementary to the Cycle 1 images.

Several complications arise in using Magellan stereo data for height determinations. First, in most regions, the SAR imaging data are projected onto a low-resolution topographic model, derived from pre-Magellan observations. This was necessary to minimize errors in location of features in regions where the elevation differed greatly from the Venus average. At a local scale, the topographic model does not affect stereo measurements, but at a regional scale, particularly in areas of large relief, height differences in the topographic model must be added to any stereo-derived height differences. A second complication is related to the geometry of the SAR observations and to the fact that all distortions occur in the **cross-track** direction. The look azimuth is generally to the east in Cycles 1 and 3 and to the west in Cycle 2, but may diverge slightly from due east or west, particularly at high latitudes. The most accurate measurements of relief-related distortion are made in the cross-track direction, which can usually be determined by plotting a line perpendicular to the edge of an orbital swath. In most Magellan mosaics, swath edges are visible either along data gaps or as "shading" artifacts. A third complication occurs when stereo measurements are to be made between orbital swaths that were processed using different spacecraft navigation solutions. These "navigation boundaries" can be identified by viewing stereo image pairs with a stereoscope. The boundary will appear

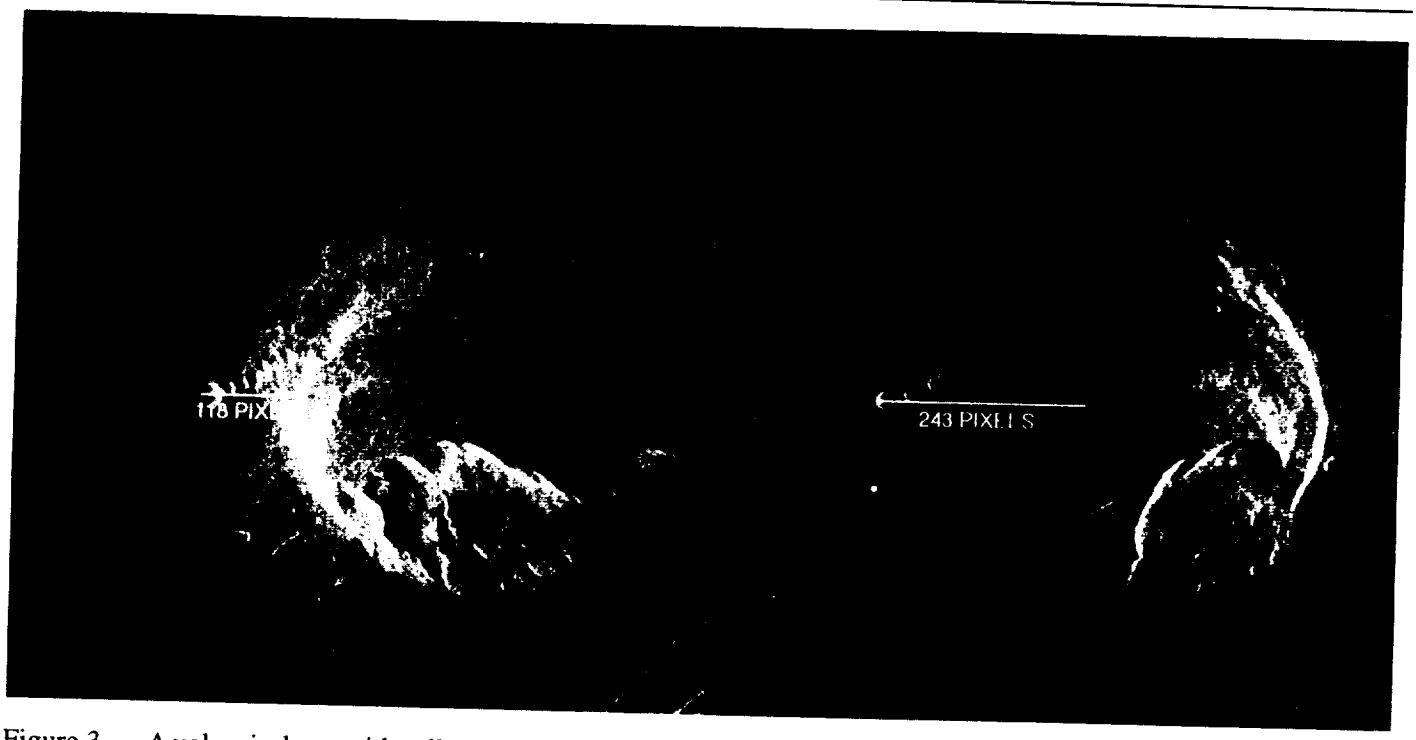

Figure 3. A volcanic dome with collapsed margins is shown in left-looking Cycle 1 data (at left) and right-looking Cycle 2 data (at right). The area shown, located at 16°S, 211.5°E, is about 60 km across. From a measurement of the parallax difference between the westernmost pit edge and the dome margin in the two images, a height difference of 2.6 km is found.

as a linear discontinuity in relief, parallel to the orbital tracks. Height determinations obtained across such boundaries are likely to be unreliable.

Applications of Stereo Analysis

The simplest way to use Magellan stereo pairs is by visual examination with a stereoscope. A stereoscope is a device that directs each image of the stereo pair exclusively to one eye. For most Magellan stereo data, the Cycle 1 image (with a large incidence angle) goes to the left eye and the Cycle 3 image (with a small incidence angle) goes to the right eye. When the images are perceived to merge, variations in relief become apparent in a 3-dimensional image. In Magellan stereo pairs, the perceived relief relative to the horizontal scale is usually about six times the actual relief (Leberl et al., JGR, 1992). For precise determinations of relief, measurements of parallax should be made on a computer monitor or on photographic enlargements (see below).

Another way to obtain a 3-dimensional view of stereo data is with color anaglyphs and 3-D color filter glasses. Standard 3-D glasses, with the red filter on the left side and the blue filter on the right, accomplish the same effect as a stereoscope by providing each image of the pair exclusively to one eye. Anaglyphs can be generated on color video monitors with Magellan digital image data. Cycle 1 data should be sent to the red channel, and Cycle 3 data should be sent to both the blue and green channels. The amount of lateral offset between the left and right images is not important, as long as the eye is able to fuse the images without too much strain.

Examples of using parallax differences to measure relief are shown in Figures 3 and 4. Figure 3 is an opposite-side full-resolution stereo pair (Cycles 1 and 2) of a scalloped dome feature at 16°S, 211.5°E. The left image, from Cycle 1, was acquired in the left-looking mode at an incidence angle of 40°. The right image, from Cycle 2, was acquired in the right-looking mode at an incidence angle of 25°. The parallax difference between the left edge of the westernmost pit and the scarp of the dome is 238 - 122 = 116 pixels. Using the formula in Figure 2, the parallax-to-height ratio for these images is 3.34. The relief can then be calculated:

$$116 \text{ pixels} \cdot (75 \text{ m/pixel})/3.34 = 2605 \text{ m}$$

This measurement is consistent with the altimeter data, which indicate that the dome summit lies 2.2 to 3.0 km above the surroundings.

Figure 4 is a same-side stereo pair (Cycles 1 and 3) of a caldera (volcanic depression) at 9.5°S, 69.0°E. The

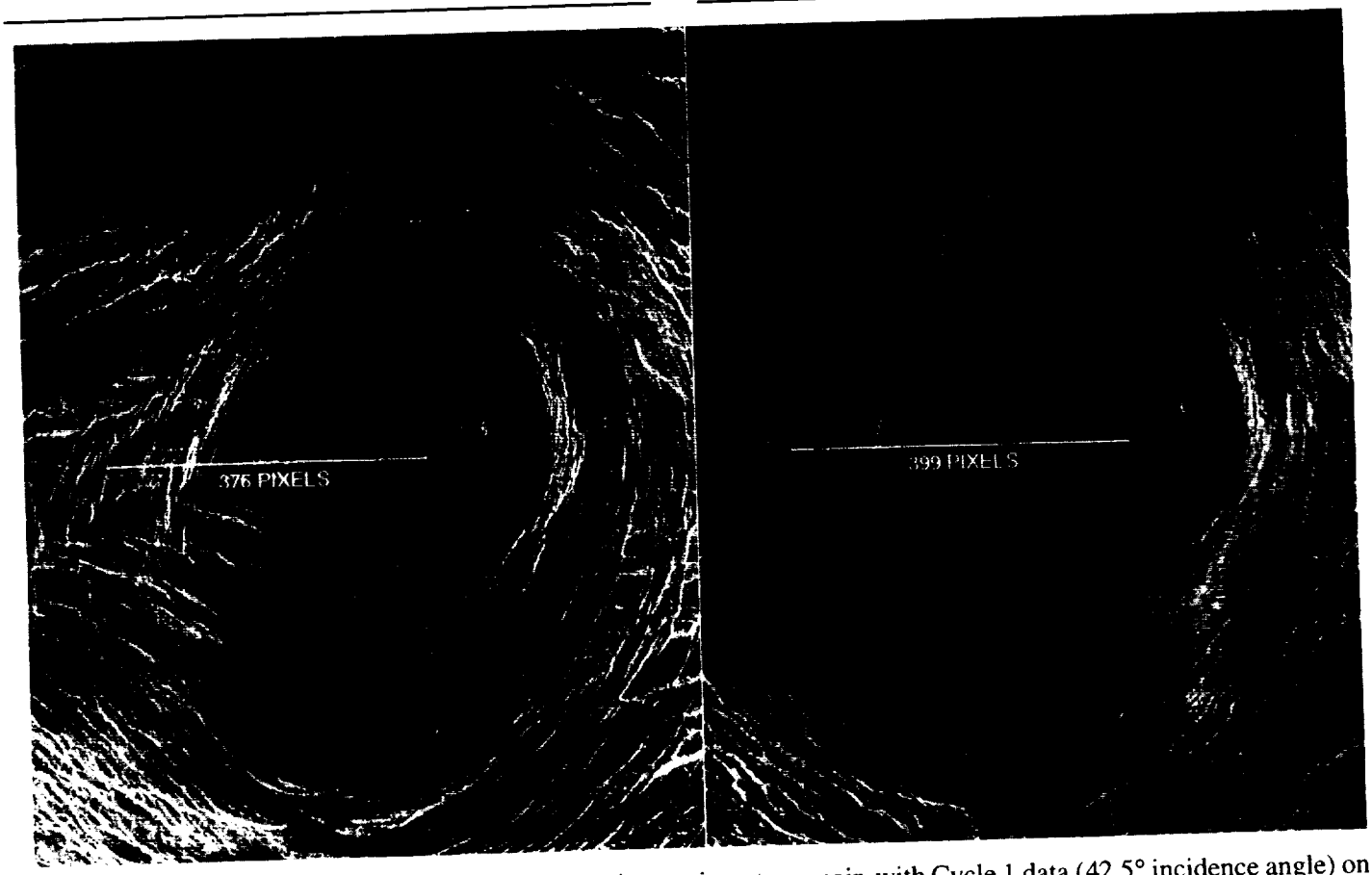

Figure 4. A caldera (volcanic pit), at 9.5°S, 69°E, is seen in a stereo pair, with Cycle 1 data (42.5° incidence angle) on the left, and Cycle 3 data (22.7° incidence angle) on the right. The images are about 60 km in width. The parallax difference between features on the rim and floor gives a depth of 1.3 km for the caldera. This image pair may be merged into a 3-D view with a stereo viewing device or by talented individuals without special equipment.

incidence angles used were 42.5° (Cycle 1, left image) and 22.7° (Cycle 3, right image). The parallax difference between features on the rim and floor of the caldera is 23 pixels. Using the formula in Figure 1, and a parallax-to-height ratio of 1.30, the relief is:

$$23 \text{ pixels} \cdot (7.5 \text{ m/pixel})/1.30 = 1327 \text{ m}$$

This is again consistent with altimeter measurements of the feature.

Digital Elevation Models

Another way that stereo images are used to derive topographic relief is through automated generation of digital elevation models (DEMs). In this technique, computer algorithms are used to match features between the two images of a stereo pair, calculate the parallax of every pixel, and generate a topographic map for the entire image. The calculation is identical to that presented above for manual derivations of heights and depths of features, but the automated DEM procedure has the advantage of producing an elevation measurement for every pixel. Topographic maps produced in this way have a lateral resolution close to the image resolution (~ 100 m), which is 100 times better than the typical resolution of the altimeter. Geologists studying the morphology (shapes) of Venusian surface features will find the DEMs extremely valuable for their analyses. Magellan has taken the "problem" of radar distortion and turned it into a stereo "solution" that greatly enhances our knowledge of the planet's surface.

References

Journal of Geophysical Research, Volume 97, Number E8, August 25, 1992, and Volume 97, Number E10, October 25, 1992.

MEETING THE TEAM

Jeffrey Plaut

Under the National Research Council's Research Associateship Program, Jeffrey J. Plaut has been doing post-doctoral research for the Magellan Science Team at JPL since May 1991. In addition to pursuing his research interests on the nature of the Venusian surface as revealed by Magellan's radar, Jeff has assisted with mission support activities such as special test planning, the MIDR (mosaic) selection process, and dissemination of Magellan science results to the public and the press.

In April 1991, Jeff received his doctorate in Earth and Planetary Sciences from Washington University in St. Louis, Missouri. The title of his dissertation was "Radar Scattering as a Source of Geological Information on Venus and Earth." His research has involved the use of remote sensing techniques and image analysis to understand the geological evolution of planetary surfaces. Field expeditions have taken him to the California and Nevada deserts, as well as to the active volcanoes on the big island of Hawaii. In his current position as a research associate at JPL, Jeff is using Magellan data to determine the nature and evolution of the geological materials exposed at the Venusian surface. Specific research topics include: surface properties and origin of Venusian volcanic deposits, impact parabolas, haloes and streaks, Magellan polarimetric radar observations, and the use of multiple views of the Venus surface (such as same-side and opposite-side stereo).

Jeff was born in Boston, Massachusetts, and attended high school in Bethesda, Maryland. He graduated from Brown University in 1980 with a Bachelor of Arts degree in music. Jeff appears at times to be obsessed with natural phenomena that affect life in southern California, such as earthquakes and the weather. His current list of hobbies includes piano, guitar, Ultimate Frisbee, tennis, and film.

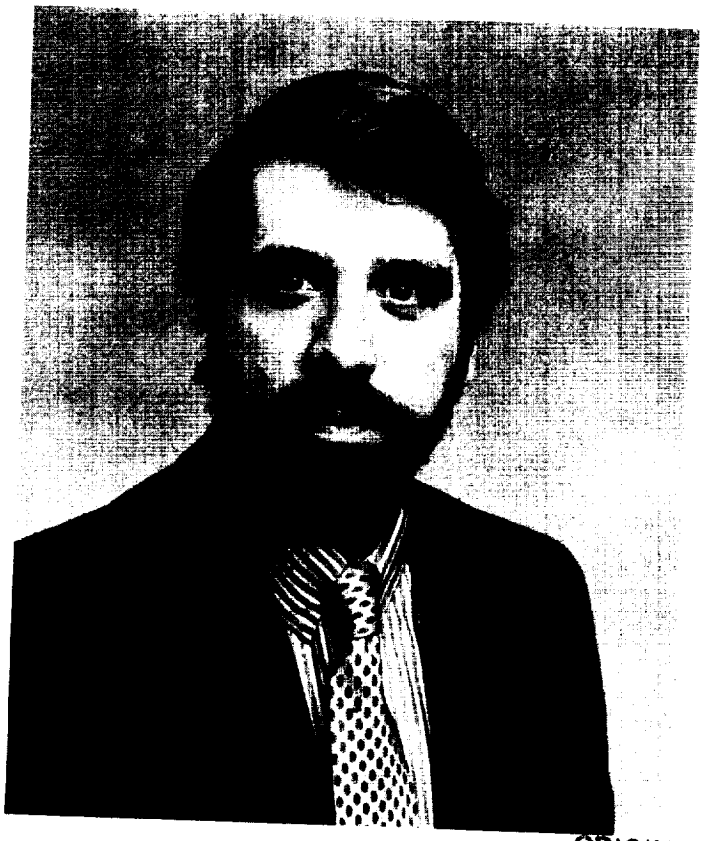

Mona Jasnow

In 1981, Mona Jasnow began working for the Venus radar mapping project, which was then the Venus Orbiting Imaging Radar (VOIR) mission. Although VOIR was short-lived and was canceled in the fall of 1981, Mona stayed with the dedicated scientists and engineers and helped to resurrect the project as the Venus Radar Mapper mission, later renamed Magellan. During this time, the project underwent many changes, not only in personnel but also in project objectives, instruments, and costs.

From June 1981 to December 1989, Mona was the project secretary for John Gerpheide, Project Manager. She was responsible for supervising the other secretaries as

well as maintaining a well-organized project office for the system managers and staff.

From January until May 1989, while the Magellan spacecraft was being readied for launch, Mona was the lead secretary for the team members at Cape Canaveral and worked as project secretary for John Gerpheide, who was Magellan's Project Manager at that time. After helping to get Magellan successfully launched, Mona assumed the duties of Administrative Assistant for science, supporting and working with Steve Saunders, Project Scientist, starting in December 1989. In that position, she was responsible for the smooth running of the science office in addition to organizing and setting up a database of all the Magellan science products. Working with the Project Scientist, she developed and implemented the Magellan Image Release Plan and has coordinated image releases.

In 1992, she became the Project Public Information Office (PIO) director, replacing Carolynn Young (who went to work for Mars Observer). In her new position, Mona is now responsible for the production of the Magellan bulletins, V-Grams, brochures, and lithos, and the coordination of PIO activities. Mona has seen the project evolve over the years and has worked with four different Project Managers as Magellan has become the immensely successful mission that mapped 98% of Earth's sister planet for the first time. Mona has been at the heart of the operation; everyone on the inside and the outside has always turned to her for information about any aspect of the Project.

Mona Jasnow was born in Cullman, Alabama. She received her Associate of Arts Degree from Pasadena City College. She has a daughter, Heather, who is a senior at Cal State Long Beach; a stepson, Todd, who is a junior at the University of Maryland; and a stepdaughter, Shari, who graduated from the University of Maryland and was recently married. Mona's husband, Ed, also works at JPL, on a defense project. In their leisure time away from the office, Mona and Ed enjoy family activities, golfing, hiking, biking, and relaxing in the warm California sun.

FINAL V-GRAM

The Magellan Project has published the V-Gram since 1980 to provide information about Venus exploration. Because of budget constraints, this will be our last issue. We hope the V-Gram has been a valuable and interesting source of information for you and your colleagues.

National Aeronautics and Space Administration

Jet Propulsion Laboratory
California Institute of Technology
Pasadena, California

JPL 410-11-20 4/93